Electrochemical and Thermal Grafting of Alkyl Grignard Reagents onto (100) Silicon Surfaces

ARTICLE *in* LANGMUIR · OCTOBER 2009

Impact Factor: 4.46 · DOI: 10.1021/la9018103 · Source: PubMed

Langmuir
Article
pubs.acs.org/Langmuir

Electrochemical and Thermal Grafting of Alkyl Grignard Reagents onto (100) Silicon Surfaces

Sri Sai S. Vegunta, Johnpeter N. Ngunjiri, and John C. Flake*

Gordon and Mary Cain Department of Chemical Engineering, Louisiana State University, Baton Rouge, Louisiana 70803

Received May 20, 2009. Revised Manuscript Received August 11, 2009

Passivation of (100) silicon surfaces using alkyl Grignard reagents is explored via electrochemical and thermal grafting methods. The electrochemical behavior of silicon in methyl or ethyl Grignard reagents in tetrahydrofuran is investigated using cyclic voltammetry. Surface morphology and chemistry are investigated using atomic force microscopy, Fourier transform infrared spectroscopy, and X-ray photoelectron spectroscopy (XPS). Results show that electrochemical pathways provide an efficient and more uniform passivation method relative to thermal methods, and XPS results demonstrate that electrografted terminations are effective at limiting native oxide formation for more than 55 days in ambient conditions. A two-electron per silicon mechanism is proposed for electrografting a single (1:1) alkyl group per (100) silicon atom. The mechanism includes oxidation of two Grignard species and subsequent hydrogen abstraction and alkylation reaction resulting in a covalent attachment of alkyl groups with silicon.

Introduction

The ability to tailor silicon surface chemistry provides key advantages for creating hybrid organic−inorganic[1,2] and biological−inorganic[3,4] devices and novel passivation methods for microelectronics processing.[5,6] Covalent silicon−carbon linkages may include various active groups (-COOH, -R-NH_2, -R-SH, and -R-OH) or passive (hydrocarbon) surface terminations. Relative to Si−H termination, Si−C bonds are relatively inert and offer improved chemical stability against oxidation since they are unpolarized and less susceptible to nucleophilic substitution reactions.[7,8]

Various methods have been adopted to create uniform and densely packed Si−C-R monolayers on silicon surfaces including: chemical,[9] thermochemical,[10] photochemical,[11] and electrochemical[12,13] routes.[14,15] Thermal routes, including hydrosilylation, typically involve precursors such as alkenes,[16] alkynes,[17] and Grignard reagents[18,19] activated by thermal treatment (catalytically or chemically promoted) or UV irradiation.[20] Electrochemical routes to direct silicon surface modification include cathodic electrografting of diazonium salts[21] or alkynes[13] and anodic electrografting of alkyl halides.[22] Grignard reagents are particularly interesting showing both thermal[23] and electrochemical[22] reactions. Previous work on thermal passivation reactions of methyl Grignards on (111) silicon surfaces show >90% surface coverage; however, the process is relatively slow (ranging from 3 h[24] to 8 days[25]) and may not fully prevent the oxidation of polycrystalline or single crystal silicon (100) surfaces. Electrografting of methyl Grignards onto silicon (111) surfaces is also shown as an efficient route to achieve fully methylated surfaces.[10,26] In this work, we examine the effectiveness of methyl and ethyl passivation of (100) silicon surfaces created via thermal and electrochemical routes.

Silicon wafers with (100) surface orientation are most commonly used in conventional microelectronics manufacturing (e.g., CMOS, NVM, and DRAM), and alternative passivation methods may reduce the use of toxic hydrofluoric acid or improve the silicon−dielectric interface quality. Furthermore, a stable surface chemistry may enable new silicon applications such as biosensors

*Corresponding author. E-mail: johnflake@lsu.edu.

(1) Faber, E. J.; de Smet, L.; Olthuis, W.; Zuilof, H.; Sudholter, E. J. R.; Bergveld, P.; van den Berg, A. *ChemPhysChem* **2005**, *6*(10), 2153–2166.
(2) Liu, Y. J.; Yu, H. Z. *ChemPhysChem* **2003**, *4*(4), 335–342.
(3) Scheibal, Z. R.; Xu, W.; Audiffred, J. F.; Henry, J. E.; Flake, J. C. *Electrochem. Solid State Lett*. **2008**, *11*(8), K81–K84.
(4) Kilian, K. A.; Bocking, T.; Gaus, K.; Gal, M.; Gooding, J. J. *Biomaterials* **2007**, *28*(20), 3055–3062.
(5) Varadan, V. K.; Varadan, V. V. *Smart Mater. Struct*. **2000**, *9*(6), 953–972.
(6) Zhu, X. Y.; Houston, J. E. *Tribol. Lett*. **1999**, *7*(2−3), 87–90.
(7) Amy, S. R.; Michalak, D. J.; Chabal, Y. J.; Wielunski, L.; Hurley, P. T.; Lewis, N. S. *J. Phys. Chem. C* **2007**, *111*(35), 13053–13061.
(8) Nemanick, E. J.; Hurley, P. T.; Brunschwig, B. S.; Lewis, N. S. *J. Phys. Chem. B* **2006**, *110*(30), 14800–14808.
(9) Schmeltzer, J. M.; Porter, L. A.; Stewart, M. P.; Buriak, J. M. *Langmuir* **2002**, *18*(8), 2971–2974.
(10) Teyssot, A.; Fidelis, A.; Fellah, S.; Ozanam, F.; Chazalviel, J. N. *Electrochim. Acta* **2002**, *47*(16), 2565–2571.
(11) Faucheux, A.; Gouget-Laemmel, A. C.; de Villeneuve, C. H.; Boukherroub, R.; Ozanam, F.; Allongue, P.; Chazalviel, J. N. *Langmuir* **2006**, *22*(1), 153–162.
(12) Koiry, S. P.; Aswal, D. K.; Saxena, V.; Padma, N.; Chauhan, A. K.; Joshi, N.; Gupta, S. K.; Yakhmi, J. V.; Guerin, D.; Vuillaume, D. *Appl. Phys. Lett*. **2007**, *90*(11), 113118(1)–113118(3).
(13) Robins, E. G.; Stewart, M. P.; Buriak, J. M. *Chem. Commun*. **1999**, No.24, 2479–2480.
(14) Shirahata, N.; Hozumi, A.; Yonezawa, T. *Chem. Rec*. **2005**, *5*(3), 145–159.
(15) Stewart, M. P.; Buriak, J. M. *Comments Inorg. Chem*. **2002**, *23*(3), 179–203.
(16) de Smet, L.; Zuilhof, H.; Sudholter, E. J. R.; Lie, L. H.; Houlton, A.; Horrocks, B. R. *J. Phys. Chem. B* **2005**, *109*(24), 12020–12031.
(17) Sieval, A. B.; Opitz, R.; Maas, H. P. A.; Schoeman, M. G.; Meijer, G.; Vergeldt, F. J.; Zuilhof, H.; Sudholter, E. J. R. *Langmuir* **2000**, *16*(26), 10359–10368.
(18) Nemanick, E. J.; Hurley, P. T.; Webb, L. J.; Knapp, D. W.; Michalak, D. J.; Brunschwig, B. S.; Lewis, N. S. *J. Phys. Chem. B* **2006**, *110*(30), 14770–14778.
(19) Yamada, T.; Shirasaka, K.; Noto, M.; Kato, H. S.; Kawai, M. *J. Phys. Chem. B* **2006**, *110*(14), 7357–7366.
(20) Takakusagi, S.; Miyasaka, T.; Uosaki, K. *J. Electroanal. Chem*. **2007**, *599*(2), 344–348.
(21) Allongue, P.; de Villeneuve, C. H.; Cherouvrier, G.; Cortes, R.; Bernard, M. C. *J. Electroanal. Chem*. **2003**, *550*, 161–174.
(22) Fidelis, A.; Ozanam, F.; Chazalviel, J. N. *Surf. Sci*. **2000**, *444*(1−3), L7–L10.
(23) Fellah, S.; Boukherroub, R.; Ozanam, F.; Chazalviel, J. N. *Langmuir* **2004**, *20*(15), 6359–6364.
(24) Yu, H. B.; Webb, L. J.; Ries, R. S.; Solares, S. D.; Goddard, W. A.; Heath, J. R.; Lewis, N. S. *J. Phys. Chem. B* **2005**, *109*(2), 671–674.
(25) Bansal, A.; Li, X. L.; Lauermann, I.; Lewis, N. S.; Yi, S. I.; Weinberg, W. H. *J. Am. Chem. Soc*. **1996**, *118*(30), 7225–7226.
(26) Fellah, S.; Teyssot, A.; Ozanam, F.; Chazalviel, J. N.; Vigneron, J.; Etcheberry, A. *Langmuir* **2002**, *18*(15), 5851–5860.

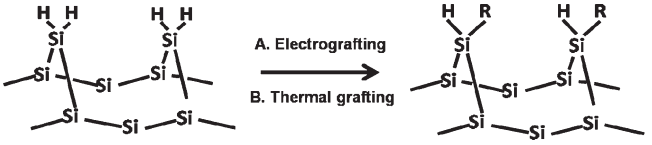

Figure 1. Passivation of H-terminated (100) silicon surface via (A) electrografting; (B) thermal grafting. R = alkyl group.

or liquid cell photovoltaics where silicon surfaces are in direct contact with biological, humid, or other aqueous environments. Figure 1 shows a schematic of alkyl monolayers on (100) silicon surfaces created via electrochemical or thermal grafting routes.

Experimental Section

Anhydrous reagents including tetrahydrofuran (THF, 99%), 3 M methylmagnesium chloride (CH_3MgCl) and 2 M ethylmagnesium chloride (C_2H_5MgCl) solutions in THF, hydrofluoric acid (HF, 48% ACS reagent), phosphorus pentachloride (reagent grade, 95%), benzoyl chloride (reagentplus, 99%), and benzoyl peroxide (reagent grade, 97%) were obtained from Sigma-Aldrich (Milwaukee, WI). Buffered Oxide Etch (BOE, ammonium fluoride/hydrofluoric acid etching mixture 6:1) and ethanol were obtained from Fisher Scientific (Pittsburgh, PA). All experiments were performed using polished *p*-type silicon wafers, 100 mm diameter with (100) orientation and resistivity ranging from 1 to 5 Ω·cm.

Silicon wafers were cleaved into 2 cm^2 square samples and immersed in BOE solutions for 30 s to yield an atomically flat silicon dihydride surface.[27,28] This procedure was followed by DI water rinsing and nitrogen drying prior to each grafting experiment. Thermal grafting and electrografting experiments were carried out in an argon atmosphere drybox system maintained with less than 1 ppm of water or oxygen.

The thermal grafting process involved heating hydride-terminated samples in benzoyl chloride solutions saturated with phosphorus pentachloride in the presence of 100 mM benzoyl peroxide at 80 °C for 40 min. Samples were subsequently washed with THF and immersed in methyl or ethyl Grignard solutions and heated at 95 °C for 8 h to obtain the corresponding methyl or ethyl termination.

Electrografting involved attaching the silicon sample to the working electrode followed by immersion into the grafting electrolyte along with a platinum counter electrode and silver wire pseudoreference. Ohmic connections were created to the backside of the silicon wafer with a GaIn eutectic. All electrochemical measurements were made without stirring and include a supporting electrolyte of 100 mM lithium hexafluorophosphate. Voltammetric experiments were performed using a Princeton Applied Research potentiostat (Model 263A). Potentials were adjusted to the Ag/AgCl reference by measuring the potential difference between the pseudoreference and the Ag/AgCl reference electrode immediately after each experiment. Samples were removed from the drybox following grafting experiments, rinsed several times with acetone and DI water, sonicated in ethanol for 5 min, then rinsed and dried prior to storage or analysis.

Infrared spectra were acquired using a Nicolet (Thermo Scientific, Madison, WI) Model 380 FTIR with an attenuated total reflectance (Spectra-Tech ATR, Model 55−390) multibounce system including a ZnSe waveguide (8 cm × 1 cm × 0.3 cm, with 45° beveled facets). The sample was pressed against the waveguide surface, while 512 scans (2 cm^{-1} resolution) were taken using a deuterated triglycine sulfate (DTGS) detector. X-ray photoelectron spectroscopy (XPS) spectra were collected on an Axis 165 photoelectron spectrometer (Kratos Analytical) with the chamber maintained at 1.5×10^{-9} Torr. An incident beam of soft X-rays (160 keV) from an Al Kα source was injected at an incident angle of 53° to the normal. AFM images were acquired using an Agilent 5400 AFM/SPM system equipped with Picoscan v5.3.3 software. *V*-shaped nonconductive silicon nitride cantilevers (MSCT-AUNM, resonance frequency 120 kHz, spring constant 0.5 N/m) were obtained from Veeco (Portland, OR), and an ambient environment was used for contact mode imaging.

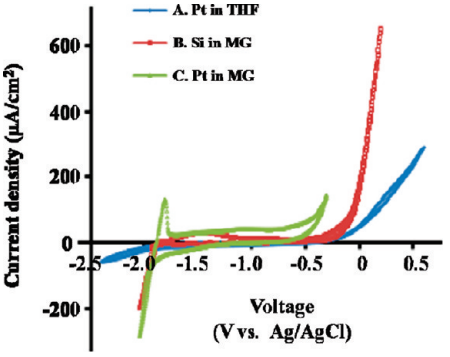

Figure 2. Cyclic voltammograms of (A) Pt working electrode in THF, (B) (100) Si−H working electrode in methyl Grignard reagent (3 M in THF), (C) Pt working electrode in methyl Grignard reagent (1 M in THF) obtained with quiescent electrolyte, at 10 mV/s scan rate (100 mM lithium hexafluorophosphate salt).

Results

Voltammetric Behavior of (100) Si in Grignard Solutions. The potential window of THF with 100 mM lithium hexafluorophosphate using a Pt working electrode is shown in Figure 2. When methyl Grignard is added to THF (1 M), the reversible Mg^{2+}/Mg couple is observed at approximately −1.9 V (vs Ag/AgCl), and the irreversible oxidation of the Grignard reagent is observed with an onset potential of approximately −400 mV (vs Ag/AgCl). When the Pt working electrode is replaced with a hydride-terminated (100) silicon sample, the Mg^{2+} reduction is consistent with the reduction potential on Pt (−1.9 V vs Ag/AgCl); however, the oxidation potential is less abrupt and shifted positively by 500 mV to −1.4 V (Ag/AgCl). Likewise, onset potential for methyl Grignard oxidation is shifted positively by approximately 300 mV on hydride-terminated silicon surfaces relative to Pt working electrodes. Oxidation of methyl Grignard occurs without significant oxidation of THF over a potential range of approximately 500 mV.

The electrochemical behavior of methyl and ethyl Grignards at (100) silicon electrodes was investigated within the anodic range from −1.4 V to 0.1 V (Ag/AgCl). As shown in the voltammograms in Figure 3A and B, methyl Grignard oxidation on (100) silicon occurs at an onset potential of approximately −0.3 V (Ag/AgCl), and ethyl Grignard oxidation on Si occurs at an onset potential of approximately −1.0 V (Ag/AgCl). As with the anodic behavior of methyl Grignard/THF solutions on Pt, methyl Grignard oxidation onset potential on (100) silicon occurs approximately 400 mV more cathodic than THF oxidation. Likewise, the onset potential for ethyl Grignard oxidation is approximately 800 mV more cathodic relative to THF oxidation. Anodic voltammetric scans of hydride-terminated surfaces with initial potentials greater than −1.9 V (Ag/AgCl), without Mg reduction, do not show significant anodic currents until Grignard oxidation is observed.

As shown in Figure 3A, the first scan in 2 M methyl Grignard solutions with an initial potential of −1.4 V (Ag/AgCl) shows an oxidation current observed at −0.4 V (Ag/AgCl). A current

(27) Buriak, J. M. *Chem. Rev.* **2002**, *102*(5), 1271–1308.
(28) Higashi, G. S.; Chabal, Y. J.; Trucks, G. W.; Raghavachari, K. *Appl. Phys. Lett.* **1990**, *56*(7), 656–658.

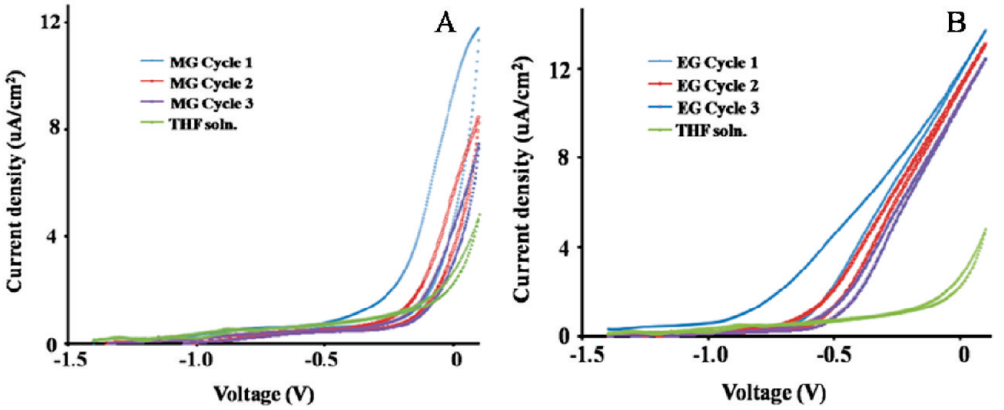

Figure 3. Cyclic voltammograms of (A) 2 M methyl and (B) 2 M ethyl Grignard reagents anodically grafted onto hydride-terminated (100) silicon wafers obtained with quiescent electrolyte, at a 10 mV/s scan rate.

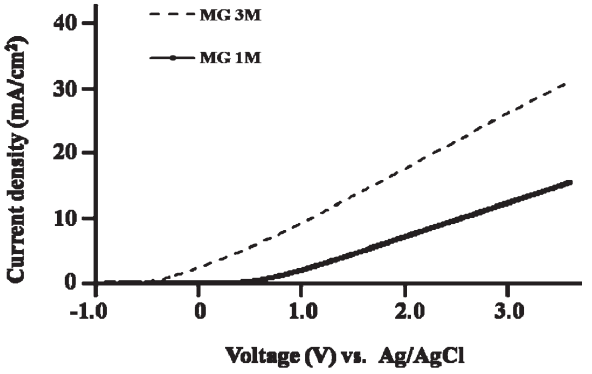

Figure 4. Voltammograms showing Grignard oxidation on a (100) silicon surface with an electrografted methyl monolayer in 3 M and 1 M methyl Grignard reagents. Quiescent electrolyte, at a 10 mV/s scan rate.

hysteresis is observed on the first and second cycles along with a positive shift in the onset oxidation of approximately 300 mV. This hysteresis and shift in the onset potential is related to the irreversible silicon surface reaction with oxidized methyl Grignard reagents and subsequent surface passivation. Similar behavior is observed for electrografting of ethyl Grignards onto (100) silicon in 2 M solutions. As shown in Figure 3B, a similar current hysteresis is observed with ethyl Grignards and the onset potential for oxidation is shifted approximately 200 mV positively in subsequent scans.

Although the voltammetric behavior of hydride-terminated (100) silicon surfaces are similar in both methyl and ethyl Grignard solutions, the onset potential for ethyl Grignard solutions is shifted approximately 500 mV cathodically relative to methyl Grignard solutions. The shift in onset potential relative to ethyl Grignards may be related to the specific oxidation potentials of these Grignard reagents.[29] As seen in the voltammetric scans shown in Figure 3, surface reactions with methyl or ethyl Grignards appear complete after the first several scans, and subsequent anodic scans show significantly diminished hystereses without shifts in onset potential.

It is also interesting to note that the oxidation of Grignard reagents continues after the surface reaction with silicon is complete. As shown in the forward scan in Figure 4, oxidation currents are dependent on Grignard concentration in THF. The current density for the anodic oxidation of methyl Grignards on grafted electrodes is approximately 15 mA/cm^2 greater in the 3 M solution relative to that in the 1 M solution. This behavior suggests that oxidation current is proportional to Grignard concentration and that products from the Grignard oxidation do not interfere with the grafted monolayer.

(29) Goebel, M. T.; Marvel, C. S. *J. Am. Chem. Soc.* **1933**, *55*, 1693–1696.

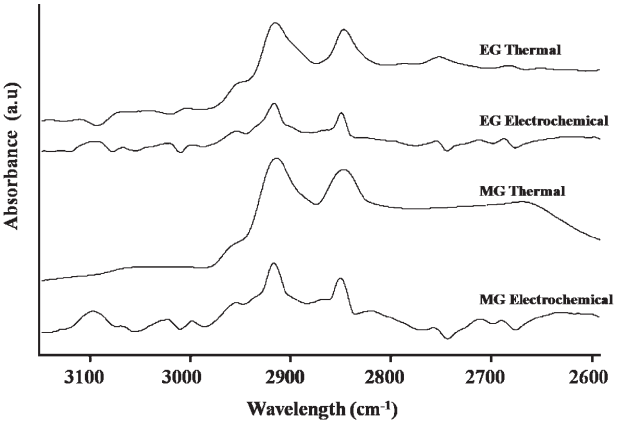

Figure 5. Absorption infrared spectra of EG (2 M ethyl Grignard) and MG (3 M methyl Grignard) grafted onto a hydride-terminated (100) silicon surface.

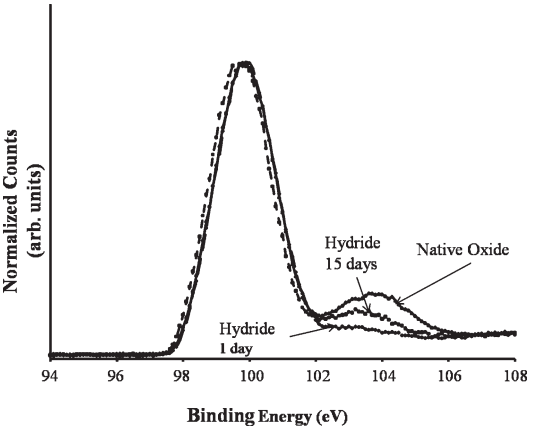

Figure 6. XPS spectra for the Si 2p region of hydride-terminated (100) silicon sample exposed for 1 and 15 days to ambient air and native oxide-terminated (100) silicon sample.

FTIR Analysis. FTIR spectra for methyl- and ethyl-terminated (100) silicon surfaces created using electrochemical and thermal grafting methods are shown in Figure 5. Infrared

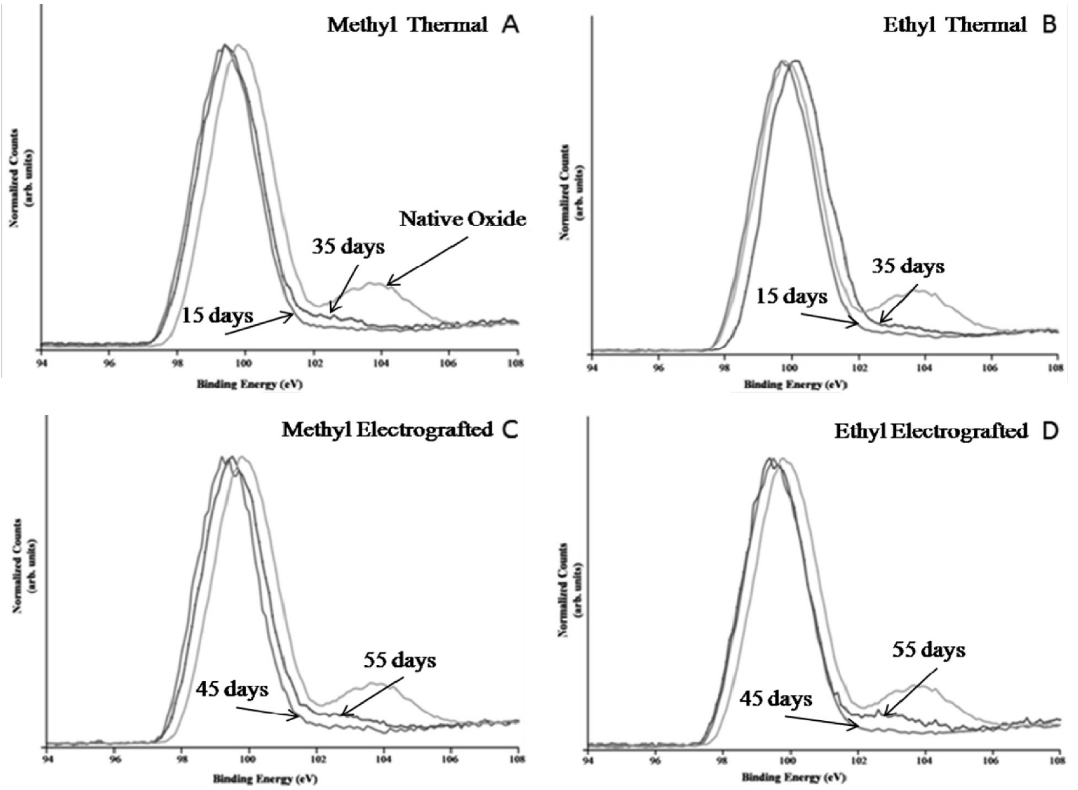

Figure 7. XPS scans of Si 2p spectra showing the passivation performance of (A) methyl thermally grafted, (B) ethyl thermally grafted, (C) methyl electrografted, and (D) ethyl electrografted onto a (100) silicon surface.

adsorption associated with carbon−carbon interactions are not detected for ethyl (or methyl)-terminated surfaces, although the C−C bond is presumed to be present in the ethyl-terminated sample. The similarity in methyl and ethyl terminations in the spectral range from 2600 to 3150 cm^{-1} is believed to be due to the crystalline alkyl environment at the surface.[25] As reported by Porter et al.[30,31] in describing the IR spectra of alkylthiols on Au surfaces, the presence of the pair of peaks at 2916 cm^{-1} (ν_a CH_2) and 2850 cm^{-1} (ν_s CH_2) also observed here, suggests that alkyl species are arranged in a crystalline structure. The shoulder at 2960 cm^{-1} is due to the asymmetric CH_3 stretch and is present in all spectra. In comparing spectra from electrografted samples with spectra from thermally grafted samples, thermally grafted samples show relatively broad peaks at 2916 cm^{-1} and 2850 cm^{-1}, whereas electrografted peaks are sharper. The broad spectra from thermal samples are similar to spectra from thermally grafted alkyl monolayers on (111) silicon surfaces with an adsorption range of 2853−2858 (ν_s CH_2) and 2921−2931 (ν_a CH_2)[31] and suggest the presence of additional methyl groups that are not arranged in the crystal methylene structure.

XPS Analysis. Silicon 2p spectra were acquired over several weeks to evaluate the stability of passivated (100) silicon surfaces after exposure to ambient laboratory conditions (~20−22 °C, 50−75% relative humidity). As shown in the XPS spectra for (100) silicon in Figure 6 (not grafted), a central Si 2p peak is observed near 99 eV, and a smaller oxygen-shifted Si 2p peak is centered at 103 eV. The Si−O peak (103 eV) intensity increases significantly after 15 days, approaching the spectra of a mature native oxide after approximately 4 weeks of ambient exposure (post HF treatment).

The Si 2p spectra for electrografted and thermally grafted (100) silicon are shown in Figure 7 along with a reference spectrum from a mature native oxide. Electrografted and thermally grafted samples were analyzed after 1, 15, 35, 45, and 55 days of exposure to ambient conditions. XPS spectra taken within the first 30 days following grafting show little variation in all samples. After 35 days of exposure in air, a small shoulder at 102 eV ($Si-O_x$) appears in the thermally grafted samples (Figure 7A and B) indicating the formation of oxides similar to 1-day old hydride-terminated samples. Electrografted samples reveal the same $Si-O_x$ shoulder at 102 eV only after 55 days of exposure in ambient conditions as depicted in Figure 7C and D. This behavior suggests that electrografted monolayers provide a greater resistance to oxidation in ambient conditions relative to that of the thermally grafted samples. In comparing the methyl and ethyl terminations, similar passivation performance is observed (effective for 55 days) showing a greater dependence on the passivation method (electrochemical versus thermal) rather than termination chemistry. The small peak at 102.8 eV present in the electrografted ethyl spectrum after 55 days of aging (Figure 7D) may also be indicative of the greater level of oxidation compared with that in similarly prepared methyl surfaces.

AFM Analysis. AFM topographs of (100) silicon surfaces electrografted with ethyl and methyl Grignards aged for 35 days are shown in Figure 8A and C, respectively. A typical monolayer can be claimed in the ethyl-terminated sample shown in Figure 8A, with the exception of a single small area of adsorbates in the 3.5 × 3.5 nm^2 image. The average rms roughness measured for the electrografted surface is 0.229 nm. A methyl monolayer produced after anodic electrografting is shown in Figure 8C and also indicates a homogeneous surface. Although imaging artifacts are present in Figure 8C, the results are consistent with a single layer of methyl functionalization obtained via electrografting.

(30) Porter, M. D.; Bright, T. B.; Allara, D. L.; Chidsey, C. E. D. *J. Am. Chem. Soc.* **1987**, *109*(12), 3559–3568.
(31) Mengistu, T. Z.; Goel, V.; Horton, J. H.; Morin, S. *Langmuir* **2006**, *22*(12), 5301–5307.

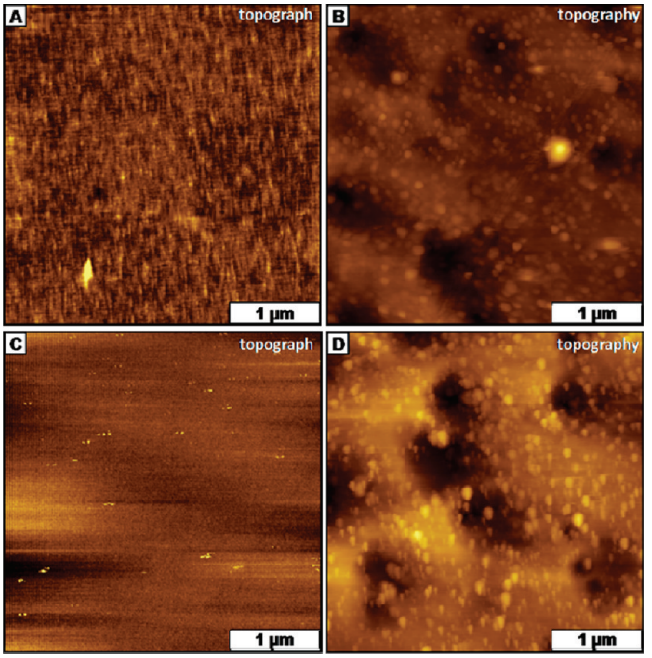

Figure 8. AFM images of passivated silicon surfaces. (A) Ethyl anodic electrografting; (B) ethyl thermal grafting; (C) methyl anodic electrografting; (D) methyl thermal grafting.

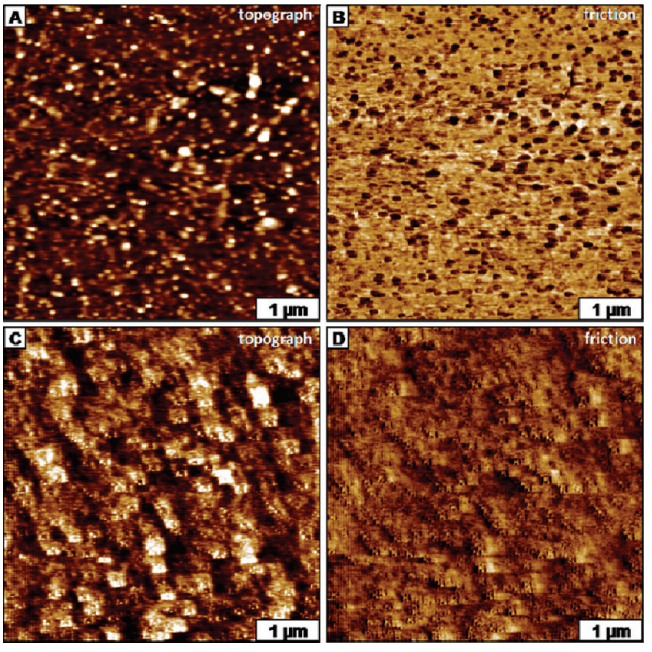

Figure 9. AFM images of thermally grafted methyl film. (A) Topographs before HF dip and corresponding (B) friction before HF dip; (C) topographs after HF dip and corresponding (D) friction after HF treatment.

The AFM topography for the thermally grafted (ethyl and methyl) surfaces (Figure 8B and D) immediately after grafting and after a series of solvent rinses reveals relatively higher levels of roughness including the presence of interspersed protrusions. Although the theoretical dimension for the upright methyl termination is 0.3 and 0.5 nm for ethyl termination, measured rms roughness for thermally grafted samples was typically greater than 10 nm. As shown in Figure 8B, rms surface roughness decreased from 10.74 to 0.72 nm after sonication in ethanol for 5 min and repeated rinsing (Figure 9A). The islands are speculated

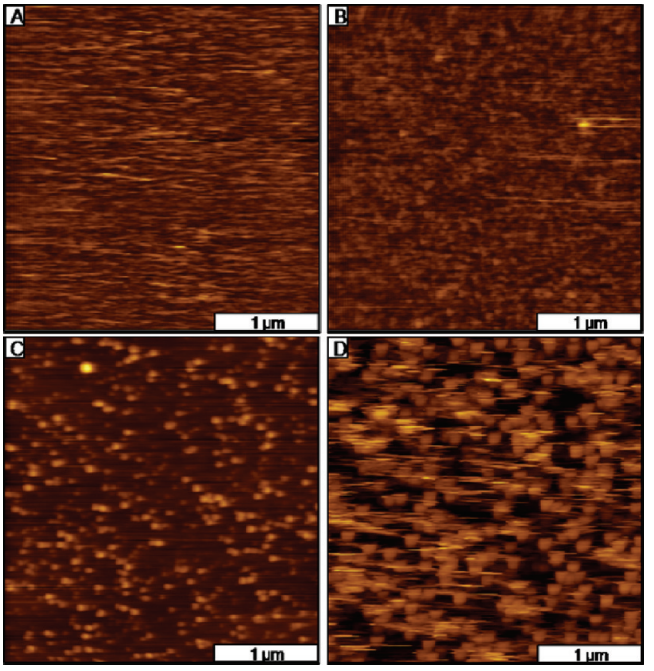

Figure 10. AFM topograph images of (100) silicon surfaces after 70 days of being electrografted with methyl; (A) before HF and (B) after HF treatment and thermally grafted with methyl; (C) before HF and (D) after HF treatment.

to be nanoscopic regions of oxides or suboxides, or organic adsorbates including reaction byproducts formed during thermal treatment. A glass slide was treated in the same methyl Grignard solution under similar conditions (3 M, 8 h at 95 °C) followed by AFM analysis to determine the origin of the adsorbates. AFM analysis revealed that similar species were present at the glass surface before and after repeated rinsing and sonication.

Thermally grafted samples such as those shown in Figure 9A with 0.72 nm rms roughness (measured after three sonication and rinse steps) were also treated with 10% HF for 5 s to evaluate native oxides as a potential origin of the elevated surface roughness. Figure 9 shows the AFM morphological difference before and after the HF dip. The triple contrast observed in Figure 9A is reduced to a double contrast (Figure 9C), which is consistent with the dissolution of silicon oxides in HF. The change in contrast after an HF dip suggests that strongly adsorbed species may remain on the surface and are not stripped in HF nor detached during sonication.[32] The multiple contrasts in the friction images (Figure 9B and D) further indicate that thermally treated samples are more heterogeneous and composed of an organic monolayer, silicon oxides, and organic adsorbates.

The AFM images shown in Figure 10 show the change in morphology before and after a 1 min 10% HF dip of a 70 day old methyl-functionalized sample (grafted via electrochemical or thermal routes). Only slight morphological changes are observed for the electrografted sample including a decrease in measured rms roughness from 0.477 to 0.163 nm after the HF dip. This may be associated with dissolution of raised oxides that may have formed at defect sites. In contrast, the rms surface roughness of thermally grafted surfaces (aged for 70 days) is increased more than 3-fold (1.46 nm before to 4.11 nm after) after HF treatment (Figure 10C and D). This behavior suggests a greater level of oxide formation, disorganized grafting, and the presence of

(32) Tsumura, M.; Ando, K.; Kotani, J.; Hiraishi, M.; Iwahara, T. *Macromolecules* **1998**, *31*(9), 2716–2723.

oligomerized species adsorbed on thermally grafted samples. As shown in Figure 10, the adsorbed species appear to remain after HF treatment suggesting that they are attached to the grafted layer rather than oxidized silicon.

Discussion

Anodic Electrografting. According to the mechanism proposed by Fellah et al.[10,26] for the anodic electrografting of alkyl Grignards on (111) silicon, the reaction proceeds via the oxidation of Grignard reagents resulting in the formation of alkyl radicals. In the subsequent electrochemical step, substitution of surface hydrogen (Si−H) by an alkyl group (R) occurs to form an active silyl species.

$$RMgX+h^+ \rightarrow [RMgX]^+ \rightarrow R^\bullet+[MgX]^+ \quad (1)$$

$$Si-H+h^+ \rightarrow Si^\bullet+H^+ \quad (2)$$

An alkyl radical ($R^\bullet$) abstracts hydrogen from the hydrogenated silicon surface.

$$H^++R^\bullet \rightarrow RH+h^+ \quad (3)$$

The activated surface ($\equiv Si^\bullet$) is expected to be strongly reactive and alkyl grafting occurs according to the final reaction step.[10,26]

$$Si^\bullet+R^\bullet \rightarrow Si-R \text{ (rate limiting step)} \quad (4)$$

As seen in the voltammetry data in Figure 3, the difference in onset potentials for ethyl and methyl electrografting on (100) silicon surfaces (approximately 600 mV) suggests that the first step toward electrografting may involve oxidation of the Grignard reagent rather than the formation of a silyl species. In this case, Grignard oxidation yields an alkyl radical which abstracts hydrogen from the dihydride (100) surface. As suggested by Fellah et al.,[10,26] another alkyl radical may subsequently react with the activated silicon surface ($\equiv Si^\bullet$) forming a covalent Si−C bond in the rate-limiting step. While complete methyl coverage of (111) surfaces may be possible, the distance between adjacent silicon atoms on (100) surfaces is approximately 4 Å, and density functional theory (DFT) calculations indicate that bond lengths of the Si−C and Si−H at an angle of 120° together constitute a length of approximately 3.5 Å.[33] Thus, the first Si−C bond formed on the (100) surface sterically hinders grafting of a second alkyl group on the same silicon site. The schematic in Figure 11 shows the mechanism proposed for anodic electrografting on (100) Si surfaces.

As shown in the proposed mechanism, the anodic reaction follows a two hole (or electron) per silicon process where both holes participate in Grignard oxidation and formation of alkyl radicals. In fact, this mechanism is in close agreement with charge estimates based on the charge hysteresis measurements shown in Figure 3. The charge difference between the forward and reverse scans on the first cycle shown in Figure 3 is 154 $\mu C/cm^2$ for electrografting with methyl Grignard and 228 $\mu C/cm^2$ for ethyl Grignard. Although the Coulombic efficiency toward electrografting reactions is unknown, these charges are comparable to the theoretical values required for complete coverage of (100) silicon (217 $\mu C/cm^2$) assuming that two holes are required for each electrografting reaction and that one alkyl is covalently bonded to each surface silicon atom.

(33) Jing, Z.; Whitten, J. L. *Phys. Rev. B* **1992**, *46*(15), 9544–9550.

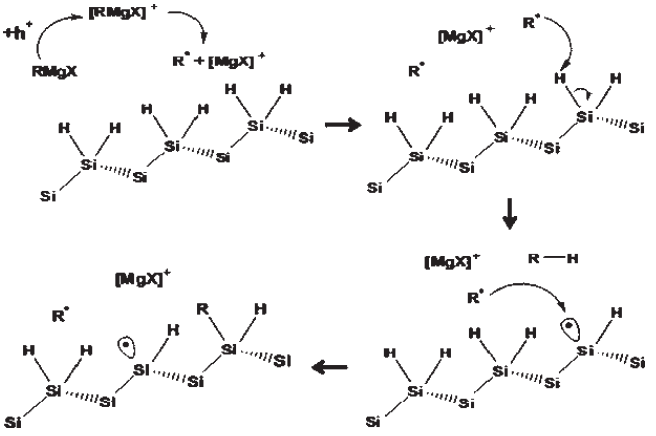

Figure 11. Schematic for the mechanism of anodic electrografting of alkyl Grignards of dihydride (100) Si surfaces.

As demonstrated here, anodic electrografting of Grignard reagents provides a direct hydride substitution process that proceeds through reactive radicals generated by the oxidative decomposition of the Grignard reagent. There is no need for an intermediate halide (i.e., Si−Cl), and the oxidation reaction is well controlled to afford a homolytic dissociation of the Grignard (RMgX ↔ R• + •MgX). In the rate-determining step, electrochemically generated radicals abstract hydrogen from the surface Si−H bond (90 kcal/mol) and form a covalently bonded Si−C surface. The process appears to be self-limiting as the electrografting reaction tends to increase the potential required to reach the same level of Grignard oxidation once the initial passivation is complete.

Thermal Grafting. As described by Lewis et al.,[18] thermal grafting procedures with Grignard solutions typically involve a chlorination pretreatment step followed by an alkylation step. On the basis of previous soft XPS results, a monochloride-terminated (100) silicon surface is obtained in an initial step with PCl_5 and chlorobenzene.[18] The chloride termination is retained during treatment in THF alone but completely replaced with alkyl groups after exposure to alkyl Grignards at 95 °C temperature for 8 h. The mechanism for the formation of a grafted monolayer on (100) silicon via this thermal route is proposed to be equivalent to the reaction on (111) surfaces where silicon passivation proceeds through the simultaneous formation of a cationic silyl species and oxidation of alkyl Grignard.[18] Subsequent steps differ greatly from electrografting pathways because of the need for an impurity from the solution (i.e., an alkyl halide reduced during Grignard oxidation) to help reduce the buildup of an interfacial energetic barrier that hinders electron injection from solution to attach the alkyl radicals to the silicon surface.[8] In contrast with methylated (111) silicon surfaces created by thermal processes, the XPS results presented here indicate that the passivation performance is relatively weaker for (100) surfaces. In addition, thermally grafted samples show relatively lower levels of passivation performance compared to that of electrografted samples. The origin of the relatively lower level of passivation observed with thermally grafted samples may be due to reduced or incomplete chlorination of dihydride-terminated silicon, incomplete alkylation of cathodic sites, or adsorbate shielding.

Steric limitations associated with (100) dihydride surface likely prevent complete chlorination (1:1 Si/Cl) as is possible with the monohydride (111) surfaces demonstrated by Lewis et al.[8,18] This partial chlorination may result in relatively lower surface alkyl coverage and decreased passivation performance of (100) surfaces relative to that of (111) surfaces. Indeed, results from

Lewis et al.[18] show that (111) surfaces thermally grafted with methyl Grignard are stable for approximately 70 days of exposure in ambient conditions, whereas the thermally grafted (100) surfaces shown in this work are stable for approximately 30 days. The incomplete chlorination of (100) surfaces may lead to regions of silicon surface which retain their dihydride termination after the thermal grafting step and are more prone to oxidation after the thermal grafting process.

Fellah et al.[23] suggest that the thermal mechanism proceeds through the formation of pools of anodic and cathodic sites in accordance with the partial chlorination of the surface. While anodic sites may undergo relatively fast alkylation, the nonchlorinated cathodic sites (with dihydride terminations) may react more slowly before complete alkylation.[26] In addition to incomplete chlorination and incomplete conversion of cathodic sites on (100) silicon surfaces, AFM results from thermally grafted samples (and from glass slides treated in the same Grignard solutions) suggest that oligomers formed during the thermal process may be strongly adsorbed to silicon surfaces and prevent complete alkylation. It is not clear if the adsorbed species preferentially affect chlorinated, nonchlorinated, anodic, or cathodic areas or if the adsorption pattern is random.

The results presented here suggest that the thermal grafting mechanism also relies on Grignard oxidation and may not require a conductive surface. In contrast with thermal methods, electrografting provides more uniform monolayers and benefits from external control of Grignard oxidation rates. As shown in the voltammetric experiments presented in Figures 3 and 4, Grignard oxidation and surface alkylation are associated with hysteresis in initial scans, and subsequent scans show increased electrode passivation without hysteresis. This passivation and shift in Grignard oxidation onset potentials results in a self-limiting electrochemical passivation process.

Conclusions

Silicon surfaces with (100) orientation are thermally and electrochemically alkylated using methyl or ethyl Grignards. Voltammetric analysis during the electrografting process shows significant hysteresis in the first anodic scan of hydride-terminated silicon in both methyl and ethyl Grignard solutions. Subsequent anodic scans show the loss of current hysteresis, and onset potentials are anodically shifted suggesting passivation of silicon surfaces. In comparison with alkyl grafting via thermal methods, electrografted samples show relatively sharper IR absorbance spectra, and AFM results show smoother surfaces. Likewise, XPS analysis of thermally and electrochemically grafted surfaces show that native oxides growth is relatively slower on electrografted samples compared to that in thermally grafted surfaces. Differences in the oxidation behavior are attributed to incomplete alkyl coverage associated with the electroless nature of the thermal grafting or adsorbate shielding. Electrografted silicon surfaces show excellent stability and are effective at limiting native oxide formation for more than 55 days in ambient conditions. This method demonstrates a facile route to the functionalization of silicon surfaces with uniform alkyl monolayers for various applications including novel microelectronic (viz. gate electrode) processing methods and new types of organic-semiconductor interfaces.